THEORETICAL CONSTRAINTS IN THE DESIGN OF MULTIVARIABLE CONTROL SYSTEMS

Final Report
NAG-1-1361

January 1993

Prepared for:
NASA Langley Research Center
Hampton, VA

Prepared by:
E.G. Rynaski
D.J. Mook

CALSPAN-UB RESEARCH CENTER P.O. BOX 400, BUFFALO, NEW YORK 14225 TEL. (716) 631-6900

TABLE OF CONTENTS

LIST OF FIGURES AND TABLES

Appendix A

ABSTRACT

The objective of the research performed under this grant was to define and investigate the theoretical constraints inherent in the design of multivariable control systems. These constraints are manifested by the system transmission zeros that limit or bound the areas in which closed loop poles and individual transfer function zeros may be placed. These constraints were investigated primarily in the context of system decoupling or non-interaction.

It was proven that decoupling requires the placement of closed loop poles at the system transmission zeros. Therefore, the system transmission zeros must be minimum phase to guarantee a stable decoupled system. Once decoupling has been accomplished, the remaining part of the system exhibits transmission zeros at infinity, so nearly complete design freedom is possible in terms of placing both poles and zeros of individual closed loop transfer functions. A general, dynamic inversion model following system architecture was developed that encompasses both the implicit and explicit configuration. Robustness properties are developed along with other attributes of this type of system. Finally, a direct design is developed for the longitudinal-vertical degrees of freedom of aircraft motion to show how a direct lift flap can be used to improve the pitch-heave maneuvering coordination for enhanced flying qualities.

1.0 Multivariable Control System Design

1.1 Introduction and Background

Future flight control systems will be designed to enhance the ability of a pilot to fly with more precision than is now generally possible. Precise flight vector control will be required for nearly every piloting task, from highly accurate approach, flare and landing to ordinance delivery, terrain following/avoidance and high angle of attack maneuvering. Most new high performance aircraft have incorporated multiple and often redundant control effectors, including canard surfaces, direct lift flaps, thrust vectoring and split rudders (ailerons) as part of the controller complement. Relatively little research has been accomplished to define how to best use these new and often novel means of generating forces and moments on the airplane to enhance the ability of the pilot to fly with maximum precision, ease and confidence.

With only one or two exceptions, aircraft flight control laws are designed on a single input-single output basis, and this approach to conceptual design served the designer well when the aircraft possessed a conventional controller complement of elevator, rudder and aileron. Because additional control effectors can provide for enhanced piloting control capability, equivalent methods of design for multicontroller configurations are needed now to provide the industry with the conceptual design tools to produce superior, multicontroller flight control system configurations.

Using conventional control surfaces, some maneuvers of an airplane are performed indirectly and are possible only because of the aerodynamics coupling inherent in the conventional geometry of an airplane. A typical example involves simple vertical plane motions - a pilot must normally rotate or pitch an airplane by elevator deflection first before an angle of attack is generated that produces a normal force enabling the airplane to maneuver (i.e., change flight path). The dynamic delay between pitching and normal force generation of a heavy, severely swept wing airplane can make it difficult for a pilot to fly (i.e., manipulate his flight path) with precision. A suitable pitch-heavy harmony must be provided. On the other hand, many aerodynamic coupling effects degrade the ability of a pilot to fly with precision. Aerodynamics coupling produces undesirable effects such as adverse/proverse yaw, dutch roll residues in the rolling response of an airplane to a pilot stick command and uncoordinated turns. The elimination of these undesirable effects often leads to decoupling or non-interaction

among the vehicle degrees of freedom of motion. Techniques of multivariable control to enhance coupling when desired and decouple when advantageous should be developed to a much greater degree than now available.

1.2 Flying Qualities Requirements

Flying qualities requirements define the satisfactory and acceptable range of static and dynamic response of an airplane to either a pilot command or to environmental disturbances. These dynamics are historically expressed in terms of frequency domain parameter ranges, such as poles and zeros of particular transfer functions with respect to stick and throttle command inputs by the pilot.

In general, all the poles of a coupled multiple degree of freedom system such as an airplane can be exactly specified, or "placed", using state feedback to a single controller. But none of the transfer function zeros can be altered, which generally means that the aerodynamics coupling among degrees of freedom of motion on the vehicle are not significantly changed by the feedback. If the airplane possesses as many independent control effectors as degrees of freedom of motion, then all poles and zeros can be exactly specified and any closed loop dynamic behavior is possible. The aerodynamic coupling among degrees of freedom of motion can be eliminated or altered at will. If the airplane possesses more than one control effector but fewer effectors than degrees of freedom of motion, then all poles and some individual transfer function zeros may be precisely specified, and are constrained by the system transmission zeros. The role of the transmission zeros is investigated in this research effort, and it is felt that much progress has been made toward the objective of better understanding and insight into the problem. This understanding is required before flight control system designers will be able to make the best use of the multiple control effectors presently being incorporated into new high performance aircraft such as the B-2 bomber, NASP (National Aerospace Plane) and the HSCT (High Speed Civil Transport).

2.0 Poles, Zeros and Decoupling

2.1 Introduction

A major objective of a flight control system design is to produce the kind of dynamic behavior that will enable the pilot to fly with precision and confidence. In order

to accomplish this design, some of the dynamics that produce undesirable aerodynamic coupling among degrees of freedom must be removed or the affects eliminated while at the same time other dynamic coupling effects should be enhanced or altered. These objectives should be attained without significantly increasing the order of the response of the aircraft through the introduction of excessive filters and compensation networks and without introducing excessive time delay.

Flying qualities requirements are most often stated in terms of frequency domain parameters, such as poles and zeros. This implies that the dynamic behavior of the vehicle, to relatively small perturbations from trim, can be described as a linear system. Because a linearized representation of the aircraft accurately represents the vehicle dynamics, the flying qualities requirements are cast mainly in linear system terms and flight control systems are successfully designed on this basis. The analysis in this report is applicable to linearized representations of the airplane, although some of the theory, such as dynamic inversion, is not restricted to a linear system representation.

2.2 Transmission Zeros and Decoupling

The zeros of a single-input, single-output transfer function constrain the area or domain of pole placement because the root locus plot involving feedback from the output is well ordered. Open loop poles will terminate at the zero locations in the s plane.

Given the linearized vehicle representation:

$$\dot{x}(t) = Ax(t) + Bu(t) \tag{1}$$

or

$$(Is-A)\, x(s) = Bu(s) \qquad \text{in the Laplace domain} \tag{2}$$

then the numerator polynomial of a transfer function is obtained using Camers' rule. A column of the control effectiveness matrix B is substituted for the appropriate column of the matrix (Is-A). The determinant of the resulting matrix yields the numerator polynomial, i.e.,

$$\begin{vmatrix} b_{11} & a_{12} \ldots & a_{1n} \\ b_{21} & s\text{-}a_{22} & \vdots \\ b_{n1} & & s\text{-}a_{nn} \end{vmatrix} = 0 \tag{3}$$

In the above example, the substitution of b_{11} for the term $s-a_{11}$ means that the numerator of the $N_{11}(s)$ transfer function will, in general be represented by a polynomial whose order is one less than the order of the denominator defined by $D(s) = |Is-A|$.

Cramer's rule can be expanded to obtain transmission zeros for multivariable as well as single input, single output systems. Partition equation 4 as shown below in such a way that B_2 is non-singular, i.e. $|B_2| \neq 0$.

$$\begin{bmatrix} \dot{x}_1(t) \\ \dot{x}_2(t) \end{bmatrix} = \begin{bmatrix} A_{11} & A_{12} \\ A_{21} & A_{22} \end{bmatrix} \begin{bmatrix} x_1(t) \\ x_2(t) \end{bmatrix} + \begin{bmatrix} B_1 \\ B_2 \end{bmatrix} u(t) \tag{4}$$

Cramer's rule can then be used to obtain the transmission zeros, which are the singularities of the polynomial

$$\begin{vmatrix} Is-A_{11} & B_1 \\ A_{21} & B_2 \end{vmatrix} = 0 \tag{5}$$

In general, the order of this polynomial is reduced from D(s) by the number of independent inputs to the system, i.e., if B is an n X 2 matrix, the order of the transmission zero polynomial will in general be n-2. If there are as many independent controllers as degrees of freedom of motion represented by Equation 1, then the system will have no finite transmission zeros.

Using Gauss' algorithm, the determinant of Equation 5 can be reduced to the expression given below:

$$\begin{vmatrix} Is-A_{11} & B_1 \\ A_{21} & B_2 \end{vmatrix} = \left|Is-A_{11}+B_1B_2^{-1}A_{21}\right| = 0 \tag{6}$$

A control law that will decouple $x_1(t)$ from $x_2(t)$ in Equation 1 is given by $u(t) = -B_2^{-1} A_{21} x_1(t) + u_C(t)$.

The application of this control law to the system of Equation 1 yields

$$\begin{bmatrix} \dot{x}_1(t) \\ \dot{x}_2(t) \end{bmatrix} = \begin{bmatrix} (A_{11}-B_1B_2^{-1}A_{21}) & A_{12} \\ 0 & A_{22} \end{bmatrix} \begin{bmatrix} x_1(t) \\ x_2(t) \end{bmatrix} + \begin{bmatrix} B_1 \\ B_2 \end{bmatrix} u(t) \qquad (7)$$

which shows that $x_1(t)$ is decoupled from $x_2(t)$, i.e., motion of $x_1(t)$ will have no effect on the response $x_2(t)$. The eigenvalues of the system of Equation 7 are given by the roots of the polynomial

$$|Is-A11 + B1\ B2^{-1}\ A21|\ |Is-A22| = 0 \qquad (8)$$

A comparison of Equation 6 and Equation 8 shows that a control law that decouples $x_1(t)$ from $x_2(t)$ places poles at the transmission zero locations of the system. Because these transmission zeros are invariant with state feedback, they, along with $|Is-A_{22}| = 0$ define the stability of a closed loop decoupled system. In order to produce a decoupled flight control system design, the transmission zeros must be minimum phase.

It appears that unstable decoupled behavior will not generally be experienced in an airplane with conventional geometry and control effectors as long as the control surfaces used do not contradict their primary purpose. For instance, to decouple pitch and heave degrees of freedom of motion from speed changes using devices designed to produce pitching moments and direct lift (i.e., elevator and direct lift flap) would not likely produce an unstable speed change dynamics. However, if $\theta(t)$ and $a(t)$ decoupling were attempted using an elevator and throttle, non-minimum phase transmission zeros are possible and perhaps likely.

2.3 Transmission and Transfer Function Zeros

The transfer function zeros of a single input system are invariant, unaffected by feedback. In a multiple input, multiple output system the transmission zeros directly affect the zeros of individual closed loop transfer functions. Because the flying qualities

of an airplane are strongly influenced by the zeros of individual transfer functions, design tools for both pole and zero placement should be developed.

Consider the two input, three output system depicted schematically in Figure 1 below:

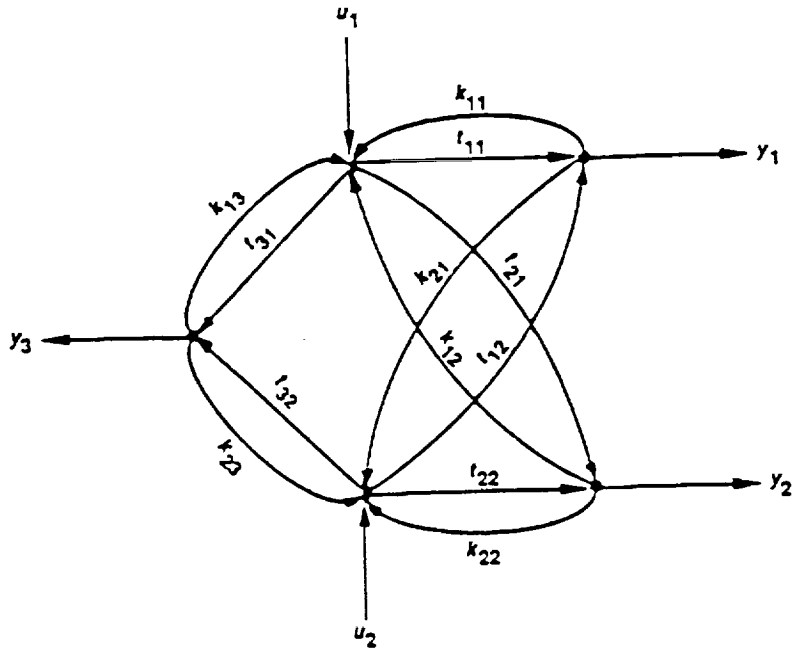

Figure 1 Conceptual 2 Input, 3 Output System

where

y_i = i^{th} output, or quantity to be fed back

u_j= the j^{th} input

t_{ij} = the open loop transfer function relating the i^{th} output to the j^{th} input

k_{ji} = the feedback function to the j^{th} input from the i^{th} output

and $tij = \frac{N_{ij}(s)}{D(s)}$ where N(s) are the numerators of the open loop transferfunctions and D(s) is the open loop characteristic polynomial

Using the rules of signal flow developed by Mason, the closed loop transfer function relating any output to any input can be written by inspection. For this system

they are

$$\frac{y_1}{u_1}(s)=\frac{N_{11}(s)+k_{22}L_1(s)+k_{23}L_2(s)}{\Delta(s)}$$
$$\frac{y_1}{u_2}(s)=\frac{N_{12}(s)-k_{12}L_1(s)-k_{13}L_2(s)}{\Delta(s)}$$
$$\frac{y_2}{u_1}(s)=\frac{N_{21}(s)+k_{21}L_1(s)+k_{23}L_3(s)}{\Delta(s)}$$
$$\frac{y_2}{u_2}(s)=\frac{N_{22}(s)+k_{11}L_1(s)-k_{13}L_3(s)}{\Delta(s)}$$
$$\frac{y_3}{u_1}(s)=\frac{N_{31}(s)-k_{22}L_3(s)-k_{21}L_2(s)}{\Delta(s)} \qquad (9)$$
$$\frac{y_3}{u_2}(s)=\frac{N_{32}(s)+k_{11}L_2(s)+k_{13}L_3(s)}{\Delta(s)}$$

where $\Delta(s)$, the closed loop characteristic polynomial is given by:

$$\Delta(s)=D(s)+\sum_{i,j} k_{ij}\ N_{ji}(s)+(k_{11}k_{22}-k_{12}k_{21})L_1(s)$$
$$+(k_{11}k_{23}-k_{13}k_{21})L_2(s)+(k_{22}k_{13}-k_{12}k_{23})L_3(s) \qquad (10)$$

and $L_1(s)$, $L_2(s)$ and $L_3(s)$ are the system transmission zeros, obtained from

$$L_1(s)=\frac{N_{11}(s)N_{22}(s)-N_{12}(s)N_{21}(s)}{D(s)}=\frac{D(s)L_1(s)}{D(s)}$$
$$L_2(s)=\frac{N_{11}(s)N_{32}(s)-N_{12}(s)N_{31}(s)}{D(s)} \qquad (11)$$
$$L_3(s)=\frac{N_{21}(s)N_{32}(s)-N_{13}(s)N_{22}(s)}{D(s)}$$

The minors $N_{11}(s)\ N_{22}(s)$ - $N_{12}(s)\ N_{21}(s)$ must contain the characteristic polynomial as a factor (ref. 1).

From the expressions given above, it can be seen that the numerators of each of the transfer functions are directly affected by two of the three transmission zero polynomials of the system, so some closed loop transfer function zero placement is

possible. Because the order of a transmission zero polynomial such as $L_1(s)$ is in general one less than an open loop numerator polynomial, the closed loop numerator polynomial can be completely specified if n-3 separate transmission zero polynomials are generated by feedback.

It is clear that the closed loop transfer function zeros, such as defined by $N_{11}(s) + k_{22} L_1(s) + k_{23} L_3(s)$ can be obtained from root locus plots involving k_{22} and k_{23}, as

$$0=1+\frac{k_{22}L_1(s)}{N_{11}(s)} \text{ and } 0=1+\frac{k_{23}L_3(s)}{N_{11}(s)} \tag{12}$$

where $L_1(s)$ and $L3(s)$ represent the invariant root locus plot zeros and $N_{11}(s)$ represent the singularities that will change as a function of the gains k_{22} and k_{23}. A direct design approach, in which the closed loop poles and zeros are selected apriori is subject to the following constraints

$$\begin{aligned} N_{11_{cl}}N_{22_{cl}}-N_{12_{cl}}N_{21_{cl}}&=\Delta(s)\, L_1(s) \\ N_{11_{cl}}N_{32_{cl}}-N_{12_{cl}}N_{31_{cl}}&=\Delta(s)\, L_2(s) \\ N_{21_{cl}}N_{32_{cl}}-N_{31_{cl}}N_{22_{cl}}&=\Delta(s)\, L_3(s) \end{aligned} \tag{13}$$

where $\Delta(s)$ is the design-objective closed loop characteristic polynomial.

Because the design method descibed above is complex, and because as many design criteria or objectives involve decoupling, the emphasis on design development methods is on decoupling, which is in itself a design objective. Direct design methods will be stressed, assuming all transmission zeros of the decoupled part of the system will be infinite. If this is so, direct dynamic inversion methods will yield the required control laws.

3.0 Dynamic Inversion, Model Following And Direct Design

3.1 Introduction

As described in Section 2.2 above, the application of the control law $u(t) = -B_2^{-1} A_{21} x_1(t) + u_C(t)$ to the partitioned system

$$\begin{bmatrix} \dot{x}_1(t) \\ \dot{x}_2(t) \end{bmatrix} = \begin{bmatrix} A_{11} & A_{12} \\ A_{21} & A_{22} \end{bmatrix} \begin{bmatrix} x_1(t) \\ x_2(t) \end{bmatrix} + \begin{bmatrix} B_1 \\ B_2 \end{bmatrix} u(t) \qquad (14)$$

will yield a closed loop system in which $x_2(t)$ is decoupled from the rest of the system. Applying the decoupling control law yields

$$\begin{bmatrix} \dot{x}_1(t) \\ \dot{x}_2(t) \end{bmatrix} = \begin{bmatrix} A_{11}-B_1B_2^{-1}A_{21} & A_{12} \\ 0 & A_{22} \end{bmatrix} \begin{bmatrix} x_1(t) \\ x_2(t) \end{bmatrix} + \begin{bmatrix} B_1 \\ B_2 \end{bmatrix} u_c(t) \qquad (15)$$

and the decoupled part of the system $\dot{x}_2 = A22\ x2(t) + B2\ u_C(t)$ can be designed completely independently as representing the dynamics of interest that will yield optimum level 1 flying qualities. The partitioning was chosen such that $|B_2| \neq 0$, so direct dynamic inversion and "exact" model following design methods are feasible.

3.2 Model Following and Dynamic Inversion

Assume that a system can be conceptually defined that yields optimum flying qualities, the model is

$$\dot{y}(t) = My(t) + B_m u(t) \qquad (16)$$

The objective is to force the plant, defined by $\dot{x}_2 = A_{22}\ x_2(t) + B_2\ u_C(t)$ to respond "exactly" as the model, defined by Equation 16. The solution is most easily and directly obtained by defining a regulator in the error between y(t) and $x_2(t)$ as

$$\dot{e}-(A_{22}+P)\ e(t)=0 \qquad (17)$$

where $\dot{e}(t) = \dot{y}(t)-\dot{x}_2(t)$ (18)

$e(t) = y(t)-x_2(t)$

and P in any stability matrix selected by the designer.

Substituting in Equation 17 for $\dot{e}(t)$ and e(t) yields

$$(\dot{y}(t)-\dot{x}_2(t)) - (A_{22}+P)(y(t)-x_2(t))=0 \quad (19)$$

Substituting one more time for $\dot{x}_2(t)=A_{22}x_2(t)+B_2u_c(t)$ yields

$$[\dot{y}(t)-A_{22}x_2(t)-B_2u_c(t)-(A_{22}+P)(y(t)-x_2(t))]=0 \quad (20)$$

Finally, solving Equation 20 above for the control input that will force $x_2(t)$ to behave "exactly" as y(t) yields the general control law

$$u_c(t)=B_2^{-1}[\dot{y}(t)-A_{22}y(t)-P(y(t)-x_2(t))] \quad (21)$$

3.2.1 Implicit Model Following

The general control law of Equation 21 above represents an entire family of solutions, depending upon the value of the matrix P selected by the designer, that will yield the same dynamic behavior of the plant. If, for instance the matrix P were chosen $P = M-A_{22}$, the control law becomes

$$u_c(t)=B_2^{-1}[(M-A_{22})x_2(t)+B_mu_m(t)] \quad (22)$$

The control law indicated by Equation 22 is shown in the block diagram of Figure 2 below. The control law involves only feedback of the states $x_2(t)$. The configuration shown in Figure 2 is often referred to as implicit model following.

Feedback is used to alter the stability and control derivatives of the plant such that the closed loop system behaves as $\dot{y}(t) = My(t)B_m u_m(t)$

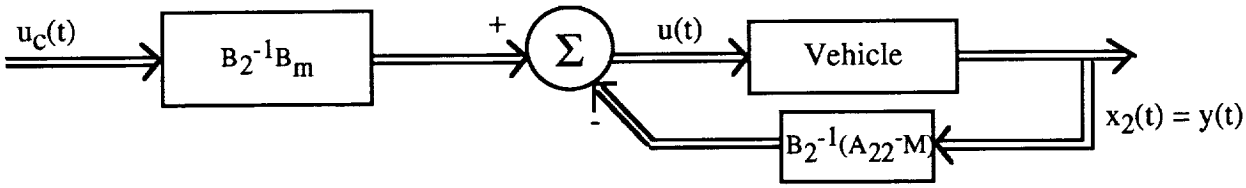

Figure 2 Implicit Model Following

3.2.2 Explicit Model Following

Since it is well known that almost anything that can be done using feedback can also be done in a feedforward sense, an alternate control law canbe obtained that does not involve feedback, simply by choosing P=0 in Equation 21. The resulting control law is given by

$$u_c(t)=B_2^{-1}[\dot{y}(t)-A_{22}y(t)] \qquad (23)$$

which represents a complete dynamic inversion of the plant, and it can then follow a model explicitly. Equation 23 above indicates that $\dot{y}(t)$ and y(t) are generated independently in a computer and the plant controllers are driven through the "gains" B_2^{-1} and $-B_2^{-1}A_{22}$ by the computer outputs y(t) and $\dot{y}(t)$.

The block diagram is shown in Figure 3 below. This architecture is often called "explicit" model following

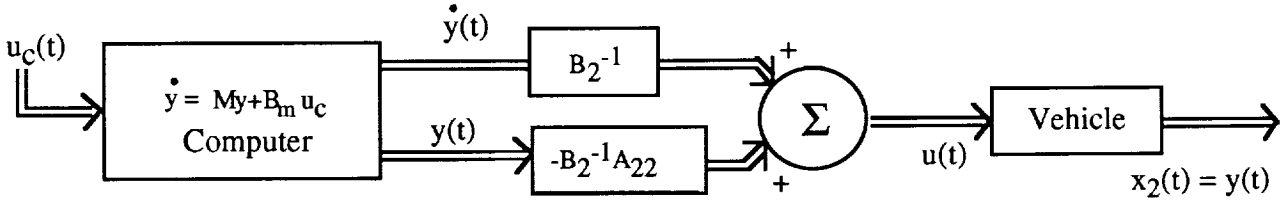

Figure 3 "Explicit" Model Following

As indicated by Equation 23 and shown in Figure 3, the configuration is entirely an open loop, feedforward architecture yet yields "exactly" the same results as shown in Figure 2, a feedback solution. The control law "gains", B_2^{-1} and $-B_2^{-1}A_{22}$ are a function only of the plant, not the model dynamics, so these gain matrices represent a complete dynamic inversion of the plant. Because this is so, the model in the computer can be changed at will without changing the control law. If, for instance, the flying qualities requirements were different for each flying task or flight regime, changing only the model dynamics will properly change the dynamic response. If the model represents a decoupled vehicle, the plant will respond as a non-interacting system.

The closed loop or feedback solution shown in Figure 2 and the open loop or feedforward solution of Figure 3 represent two extremes of a family of solutions that can be obtained that produce equivalent dynamic inversion results, therefore, a complete model following capability. There is no control law uniqueness. For instance, consider the feedforward or open loop solution of Equation 23.

$$u_c(t)=B_2^{-1}[\dot{y}(t)-A_{22}y(t)] \tag{23}$$

which drives the plant through the generation of $\dot{y}(t)$ and $y(t)$. Two other variations of this same control are easily obtained. A second control law is obtained by substituting for $\dot{y}(t)$ in Equation 23 above.

$$u_c(t)=B_2^{-1}[(M-A_{22})y(t)+B_m u_m(t)] \tag{24}$$

This control law strongly involves the computer model dynamics, so as the model dynamics are changed, the control law also changes. The block diagram is shown in Figure 4 below.

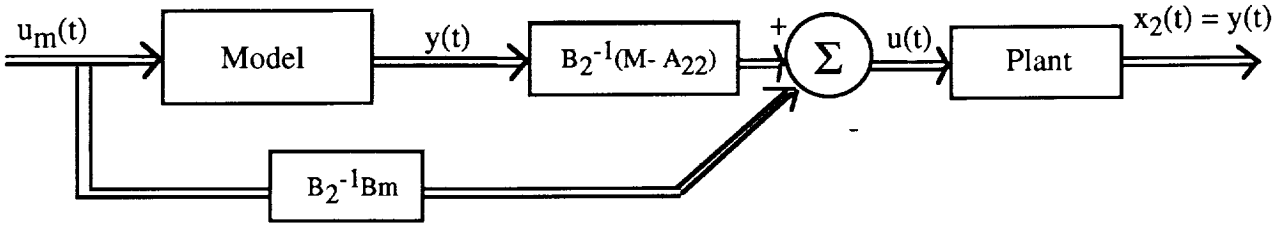

Figure 4 Alternate "Explicit" Model Following Architecture

Because M and A_{22} are matrices of dimensional stability derivatives and if the model is considerably more stable than the plant, i.e., if $M >> A_{22}$ then the solution is relatively independent of the plant stability derivatives but still strongly a function of the plant control effectiveness terms or stability derivatives.

A third architecture of the explicit model following control law is given by

$$u_c(t)=B_2^{-1}\left[\left(I-A_{22}M^{-1}\right)\dot{y}(t)+A_{22}M^{-1}B_m u_m(t)\right] \tag{25}$$

This control law reduces simply to $u(t)=B_2^{-1}B_m u_m(t)$ if the matrix of stability derivatives of the plant and the model are identical.

In summary, because there are three vectors $\dot{y}(t)$, $y(t)$ and $u_m(t)$ of the model and any two are required for the model following task, control laws are not unique. In fact, feedforward and feedback "hybrid" control law architectures can also be easily obtained. Consider the following single controller example given below in which it is desired to have an aircraft whose (two degree of freedom) $q/d_e(s)$ transfer function is given by

$$\frac{q}{\delta e}(s)=\frac{k(s+1/\tau_{\theta_2})}{s^2+2\zeta\omega s+\omega^2} \tag{26}$$

and it is desired to have the vehicle respond in pitch rate as the model

$$\frac{q_m}{\delta e}(s)=\frac{k_m(s+1/\tau_m)}{s^2+2\zeta_m\omega_m s+\omega_m{}^2} \tag{27}$$

This behavior can be obtained by cascading a lag-lead (or lead-lag) filter model as a prefilter, then using pitch rate feedback and an observer to alter the characteristic polynomial. The system becomes as shown below in Figure 5.

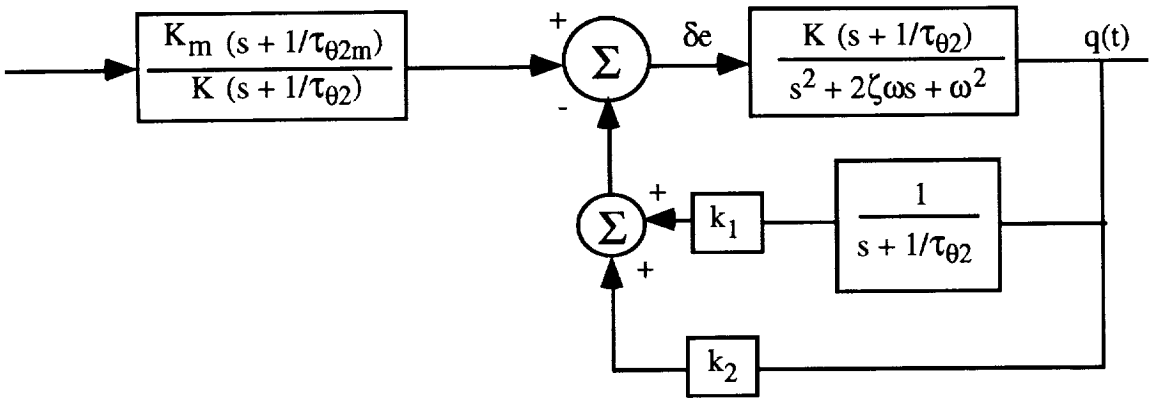

Figure 5 Single Controller "Model Following"

where k_1 and k_2 are obtained from

$$s^2+2\zeta\omega s+\omega^2+k_2k(s+1/\tau_{\theta_2})+k_1k=s^2+2\zeta_m\omega_m s+\omega_m{}^2 \qquad (28)$$

or, equating powers of s

$$2\zeta\omega+k_2k+k_1k=2\zeta_m\omega_m \qquad (29)$$
$$\omega^2+k_2k/\tau_{\theta_2}+k_1k=\omega_m{}^2$$

It is clear that although the pitch rate of the aircraft is made to "follow the model" using a hybrid feedforward-feedback architecture, the procedure involved characteristics of both pitch rate and angle of attack. If this procedure were used to "simulate" the dynamics of one airplane using another as the plant, the simulation would not be accurate because the more important maneuvering dynamics represented by a(t) would be incorrect and would be "higher order," generally detrimental to flying qualities. In general, it is not possible to adequately emulate the short period dynamics of a different aircraft unless both a pitching moment and direct lift effector were used.

3.2.3 General Solution

As indicated in Equation (23) and shown in fig. 3, the feedforward model following configuration is entirely an open loop architecture, yet yields "exactly" the same result as shown in fig. 2, a feedback solution. The control law "gains", B_2^{-1} and $B_2^{-1}A_{22}$ are a function only of the plant, and these gains constitute a complete dynamic

inversion of the decoupled part of the plant. Because this is so, the model in the computer can be changed at will without changing the control law in any way. If, for instance, the flying qualities requirements were different for each flying task or flight regime, changing only the model dynamics will properly change the dynamic response. In fact, a ground-based simulator operates in exactly the way described above. The only difference is that the airplane is moving, not standing still, so the velocity and dynamic pressure dependent derivatives A_{22} are finite and must be taken into account.

The closed loop or feedback solution of fig. 2 and the open loop or "feedforward" solution of fig. 3 represent two extremes of the family of solutions that can be obtained. Neither system is particularly robust in the sense that flight condition variations of the stability and control derivatives B_2 and A_{22} will cause deviations in the desired response unless a lot of gain scheduling is used. Even with gain scheduling, the lack of low frequency robustness of the system shown in fig. 3, would preclude its use in an actual airplane. However, robustness can be easily provided and in fact, the system shown in fig. 3, with feedback added, can result in a robust architecture, accounting for the variation of the stability and control derivatives of B_2 and A_{22}. In fact, there is reason to believe, as shown below, that minimal gain scheduling is possible for many aircraft.

The family of solutions that will yield a robust system configuration is given by the general solution of Equation (21). The block diagram of the system represented by Equation (21) (including the decoupling feedback) is shown in fig. 6 below:

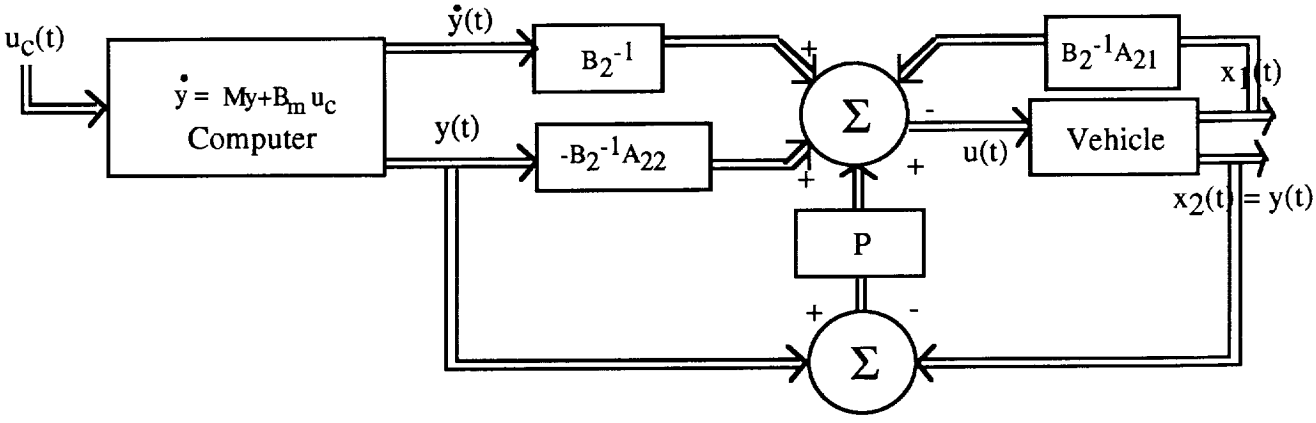

Figure 6 General "Model Following" Control System

The general solution of Equation (21), (i.e., fig. 5), shows that the matrix P acts on the error between the desired output y(t) and the actual output $x_2(t)$. If B_2 and A_{22} are known "exactly", the error is zero and P has no function. In fact, P defines not only the regulation of the error between y(t) and $x_2(t)$ but also defines the perturbation response of $x_2(t)$ to external disturbances (gust alleviation). Most importantly, because P can be an integration process, low frequency robustness can be provided, so the response of the computer output and the aircraft output will not diverge. Because all the flying qualities requirements can be resident in the computer model, gust alleviation or structural mode control functions can be done using feedback without affecting the maneuvering flying qualities requirements. In fact, Equation 21 is simply a formalization of the present common practice of providing feed forward gains in a flight control design.

If the computer is programmed such that the kinematics of the plant are resident in the computer but the aerodynamics in the computer are chosen for flying qualities purposes, the computer can represent a global "model following" system. If such a system were used for a wide flight range vehicle such as HSCT, the HSCT vehicle would always be at the same flight condition as the computer generated "model," but the HSCT vehicle would respond dynamically as the "level 1" flying qualities model. There is reason to believe that the configuration defined by fig. 6 would work well for a wide flight range vehicle.

Because the function P acts on the error between the computer generated model response and the actual vehicle response, P can represent a robust compensator as defined by such methods as an H_∞ system designed to minimize the error as the stability and control derivatives A_{22} and B_2 vary with flight condition.

In general, any compensation network can be expanded in partial fraction expansion form to represent proportional, integral and derivative components (or designed as a PID system). To show how such a network could be designed for an architecture of this type, consider a PID system, resulting in an error control law.

$$u_e(t) = -K_1 e(t) - K_2 \int e(t)dt - K_3 \dot{e}(t) \qquad (30)$$

shown in fig. 7 below:

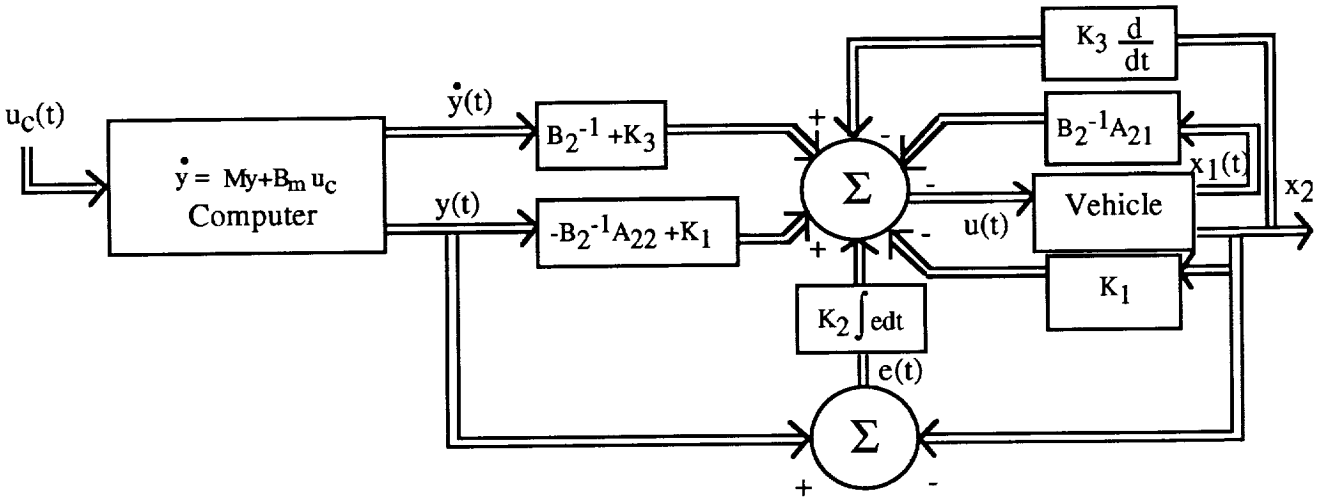

Figure 7 Robust Model Following Architecture

This block diagram is drawn to highlight the effects of the PID feedback and the effect of this feedback on the response of the system as stability and control derivatives B_2 and A_{22} vary in flight. As shown in the figure, the accuracy of the design depends upon the accuracy of B_2 and A_{22}, the matrices involved in the dynamic inversion. If the feedback gains are made sufficiently large, the system can be made insensitive to variations in the stability and control derivatives, i.e.,

if $K_3 >> B_2^{-1}$	Æ insensitive to variations in control effectiveness and in control surface nonlinearities
if $K_1 >> -B_2^{-1} A_{22}$	Æ insensitive to variations in $B_2^{-1} A_{22}$, i.e., the stability derivatives

Making the fair assumption that the feedback is to maintain or improve the stability of the vehicle, the integral of the error will guarantee $x_2(t) = y(t)$ in the long term, regulating always about the trajectory of the airplane on the model computer (for instance, a hypersonic NASP with ideal level 1 flying qualities) without the need to directly measure some air data (such as velocity) on the vehicle itself. Because the integral guarantees long term zero error, the pilot command input-response output is independent of flight condition and can be made constant or vary with flight condition exactly as specified (Fs vs. n_z) in the F.Q. specifications. Because in the long term the aircraft steady state response will be totally predictable, a display of the pilot command

input will tell the pilot what the steady state flight variable changes will be regardless of the sluggishness of the vehicle response, resulting in a "predictor" display. By limiting commands at the model, functions such as angle of attack and sideslip can be limited, again useful for a NASP system. The problem solving potential of this type of system architecture seems significant.

Even more advantages for this architecture can be realized. For instance, because the gains $B_2^{-1} A_{22}$ represent a "division" process of dimensional stability and control derivatives, many of which are dimensionalized in exactly the same way, many of the terms of $B_2^{-1} A_{22}$ are simply (constant) ratios of non-dimensional stability derivatives, such as $c_{m_a}/c_{m_{d_e}}$, which can be accurately obtained in a wind tunnel. These constants occur along the diagonal of the matrix $B_2^{-1} A_{22}$, so the robustness oriented gains would be designed to minimize the effects of off-diagonal terms, (if their effect is significant). Because the aircraft can be made to respond to disturbances entirely independently of the computer model (which doesn't respond at all unless turbulence is measured and injected into the computer), the feedback can be tailored for gust alleviation or structural mode control or even to minimize wing root bending moments (to disturbances) without affecting flying qualities (resident in the computer). The minimization of maneuver loads can be dealt with in the model computer and reflected in the vehicle itself. For instance, if the "model" had a direct lift flap, along with the vehicle, distribution of "model" wing loads would be reflected in the vehicle itself.

3.3 Direct Design Methods

Because the decoupling described in Section 2.2 was done in such a way that the partitioned matrix B_2 was non-singular, the remaining system $\dot{x}_2(t)=A_{22}\, x_2(t)+B_2 u_C(t)$ has no transmission zeros and every element of $x_2(t)$ can be exactly "placed," i.e, both poles and zeros can be specified. This is shown by an example in this section.

One of the more important objectives of a Level 1 flight control system design is to provide for good pitch/heave harmony in the sense that if the pitch rate and angle of attack responses are similar, then the difference between rate of change of attitude and rate of change of flight path angle is minimized. The airplane will dynamically "curve" a path through the sky. Since $\dot{\alpha} \doteq q+Z_\alpha \alpha$, then $\dot{\gamma}=q-\dot{\alpha} \doteq -Z_\alpha \alpha$ and the rate of change of flight path angle is directly proportional to change in angle of attack. Therefore, if the pitch

rate response is very similar to the angle of attack response, the flight path and pitch responses are in harmony.

Pitch rate and angle of attack vehicle responses are dominated by the two degree of freedom short period mode. However, flight precision requires not only attitude/angle of attack harmony in the short period mode, but the phugoid mode as well. If the phugoid dynamics were decoupled from the pitch rate and angle of attack responses, the altitude/flight path angle harmony is maintained with precision beyond the short term response of the vehicle.

Speed change or phugoid dynamics will not affect the angle of attack/pitch rate response if velocity changes were decoupled from the rest of the system. If speed changes were decoupled, as defined by Equation 7, the subsystem $\dot{x}_2(t)=A_{22}x_2(t)+B_2u(t)$ can be represented by the remaining two degree of freedom dynamics

$$\begin{bmatrix} \dot{q}(t) \\ \dot{\alpha}(t) \end{bmatrix} = \begin{bmatrix} M_q & M_\alpha \\ 1 & Z_\alpha \end{bmatrix} \begin{bmatrix} q(t) \\ \alpha(t) \end{bmatrix} + \begin{bmatrix} M_{\delta e} & Z_{\delta e} \\ M_{\delta z} & Z_{\delta z} \end{bmatrix} \begin{bmatrix} \delta_e(t) \\ \delta_z(t) \end{bmatrix} \tag{31}$$

where d_e and δ_z represent deflections of an elevator and direct lift flap (or other direct lift force effector). With suitable interconnections to produce force and moment decoupling, this equation can be simplified

$$\begin{bmatrix} \dot{q}(t) \\ \dot{\alpha}(t) \end{bmatrix} = \begin{bmatrix} M_q & M_\alpha \\ 1 & Z_\alpha \end{bmatrix} \begin{bmatrix} q(t) \\ \alpha(t) \end{bmatrix} + \begin{bmatrix} M'_{\delta e} & 0 \\ 0 & Z'_{\delta z} \end{bmatrix} \begin{bmatrix} \delta_{e_c}(t) \\ \delta_{z_c}(t) \end{bmatrix} \tag{32}$$

The objective will be to define a control law

$$u(t)=-k_1x(t)+L\delta_{stick}(t) \tag{33}$$

such that the closed loop system will have a specified closed loop short period frequency and damping ratio and the numerators of the $\alpha/\delta_s(s)$ and $q/\delta_s(s)$ transfer functions will have the same or approximately the same numerator zero. If the feedforward gains L are designed such that the pilot commands the elevator and direct lift flap together, the closed loop system is defined as

$$\begin{bmatrix} \dot{q}(t) \\ \dot{\alpha}(t) \end{bmatrix} = \begin{bmatrix} M_q - M_{\delta e}k_{11} & M_\alpha - M_{\delta e}k_{12} \\ 1 - Z_{\delta z}k_{21} & Z_\alpha - M_{\delta z}k_{22} \end{bmatrix} \begin{bmatrix} q(t) \\ \alpha(t) \end{bmatrix} + \begin{bmatrix} M_{\delta e} \\ Z_{\delta z} \end{bmatrix} \delta_s(t) \qquad (34)$$

The problem is then arranged with four available feedback gains k_{11}, k_{22}, k_{12} and k_{21} to obtain the short period frequency, damping ratio and numerator zeros desired. The closed loop transfer function will have the form

$$\frac{\alpha}{\delta_s}(s) = \frac{C_1(s-z_1)}{s^2+2\zeta\omega s+\omega^2} \qquad (35a)$$

$$\frac{q}{\delta_s}(s) = \frac{C_2(s-z_2)}{s^2+2\zeta\omega s+\omega^2} \qquad (35b)$$

where and z_1, z_2, ω and ζ are to be attained using feedback.

The closed loop system of Equation 34 is of the form

$$\begin{bmatrix} \dot{\alpha}(t) \\ \dot{q}(t) \end{bmatrix} = \begin{bmatrix} a_{11} & a_{12} \\ a_{21} & a_{22} \end{bmatrix} \begin{bmatrix} \alpha(t) \\ q(t) \end{bmatrix} + \begin{bmatrix} b_1 \\ b_2 \end{bmatrix} \delta_s(t) \qquad (36)$$

whose characteristic polynomial and numerator transfer function polynomials are given by

characteristic polynomial:

$$\begin{aligned} \Delta(s) &= s^2+s(-a_{11}-a_{22})+a_{11}a_{22}-a_{12}a_{21} \\ &= s^2+2\zeta\omega s+\omega^2 \end{aligned} \qquad (37)$$

numerator polynomial:

$$N_\alpha(s) = b_1(s-a_{22}+\frac{b_2}{b_1}a_{12}) = b_1(s-z_1) \quad (38a)$$

$$N_q(s) = b_2(s-a_{11}+\frac{b_2}{b_1}a_{21}) = b_1(s-z_2) \quad (38b)$$

If $z_1=z_2$, then $N\dot{\gamma}(s)=-Z_\alpha N_\alpha(s)=-Z_\alpha b_1(s-z_1)$, so the dynamic response of $\dot{\gamma}$ and q differs only by a constant.

From Equation 36, each of the closed loop elements a_{11}, a_{12}, a_{21}, and a_{22} can be obtained in terms of the specified poles, zeros and control effectiveness terms as

$$a_{22} = \frac{\omega^2+2\zeta\omega z_1+z_1z_2}{z_2-z_1} = Z_\alpha - Z_{\delta_e}k_{22} \qquad k_{22} = \frac{Z_\alpha - a_{22}}{Z_{\delta_e}} \quad (39a)$$

$$a_{11} = a_{22}-2\zeta\omega = M_q - M_{\delta c}k_{22} \qquad k_{11} = \frac{M_q - a_{11}}{M_{\delta_e}} \quad (39b)$$

$$a_{12} = \frac{b_1}{b_2}(a_{22}-z_1) = M_\alpha - M_{\delta c}k_{12} \qquad k_{12} = \frac{M_\alpha - a_{12}}{M_{\delta_e}} \quad (39c)$$

$$a_{21} = \frac{b_2}{b_1}(a_{11}-z_2) = 1-Z_{\delta_e}k_{21} \qquad k_{21} = \frac{1-a_{21}}{Z_{\delta_e}} \quad (39d)$$

The resulting configurations is exactly in the form of an implicit model following solution. The only constraint is that z_1 cannot equal z_2 because element a_{22} would be required to be infinitely large. Other than this, there appears to be no reason why complete pole-zero placement cannot be achieved and design criteria attained.

The feedback methods used are state feedback methods that directly alter stability derivatives. Therefore, the order of the system open loop and closed loop is theoretically the same and no higher order dynamics or time delay has been deliberately added to the system, therefore having no detrimental effect on the flying qualities. Because the

stability and control derivatives can be directly related to the frequency domain format of the flying qualities requirements, the technique described above can be used to design directly to the flying qualities specifications.

Direct design techniques to satisfy flying qualities and precision control criteria are still in a stage of initial development, although much progress, as shown in this report, has been made. The results shown above demonstrate a specific rather than a totally general solution. The ultimate goal of the research is to provide for a completely general solution that can be extended to vehicles having many degrees of freedom of motion, such as aeroelastic well as rigid body vehicle motions. Although the signal flow oriented methods of Section 2 could have been successfully used to accomplish the results shown above, it is felt that the complexity of the signal flow methods warrants development of direct design methods.

4.0 References

1. Rynaski, E.G. and Ball, J.N., "Longitudinal Flight Control for Military Aircraft - A Study of Requirements and Design Concepts," Cornell Aeronautical Laboratory Report ID-1757-F-1, October 1963.

APPENDIX A
Flight Simulation Derivation

The theoretical developments of the transmission zero work performed under this agreement were tested on a simulation of pitch-heave maneuvering coordination for enhanced flying qualities. This appendix explains the development of the simulation used in the numerical testing.

The computer simulations represent the experimental Total In Flight Simulator (TIFS) aircraft, operated by the CALSPAN Flight Research Department.

For simulation purposes, the TIFS is assumed to be flying as a rigid body in a vertical (longitudinal) plane, so that there are three degrees-of-freedom (horizontal translation x, vertical translation z, and pitch angle θ). Aerodynamic coefficients are consistent with CALSPAN reports. The details of the simulation follow.

Coordinate Systems

In developing the aircraft equations of motion, two different coordinate systems are used, shown in Figure 1. One is an inertial coordinate system, which is fixed to the earth and is considered to be a non-rotating system. This is a valid assumption since the rotation of the earth is negligible in most aircraft dynamic problems. The other system is fixed to the aircraft center of gravity and rotates along with the aircraft. This system is referred to as the body axis coordinate system.

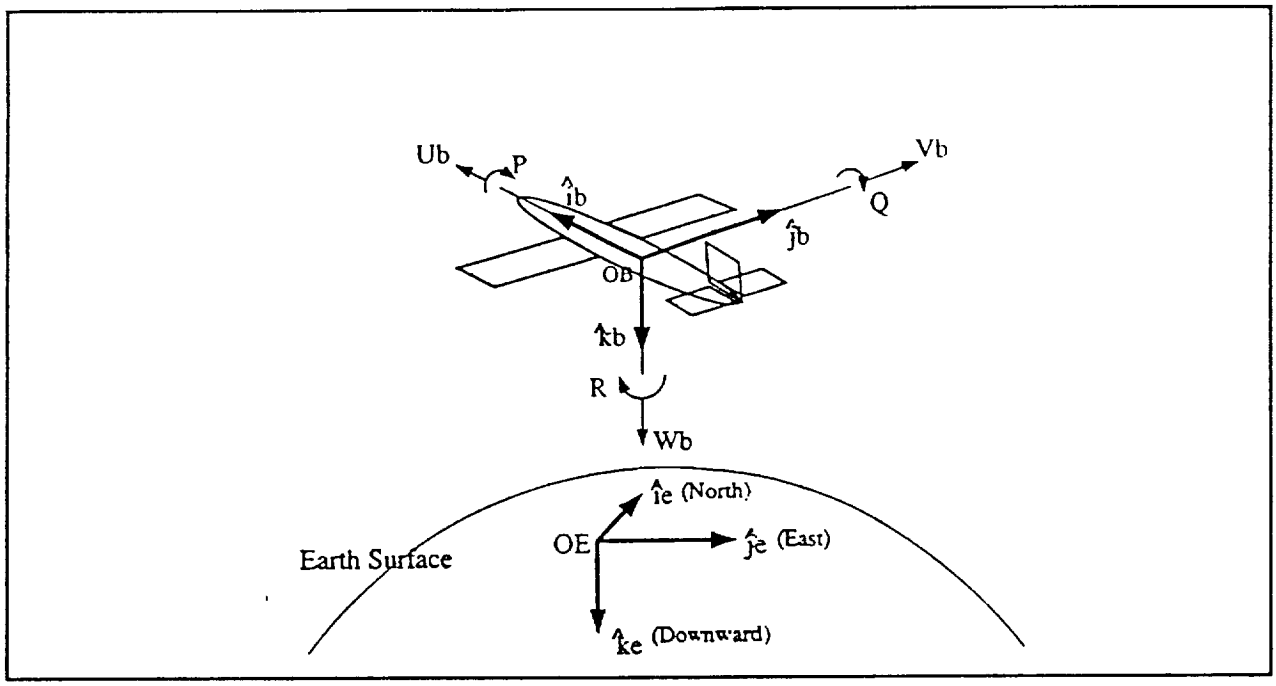

Figure 1 Coordinate Axis System

Equations of Motion

Newton's second law is used to derive the rigid body equations of motion, i.e., the conservation of both linear and angular momentum (Nelson [2]):

$$\sum \vec{F} = \frac{d}{dt} \sum (m\vec{v}) \tag{1}$$

$$\sum \vec{M} = \frac{d}{dt}\vec{H} = \frac{d}{dt} \sum \vec{r} \times m\vec{v} \tag{2}$$

The airplane is considered as a continuum of mass particles (δm) and each elemental mass has a velocity ($\vec{v}$) relative to an inertial frame. Newton's second law is:

$$\delta\vec{F} = \delta m \frac{d\vec{v}}{dt} \tag{3}$$

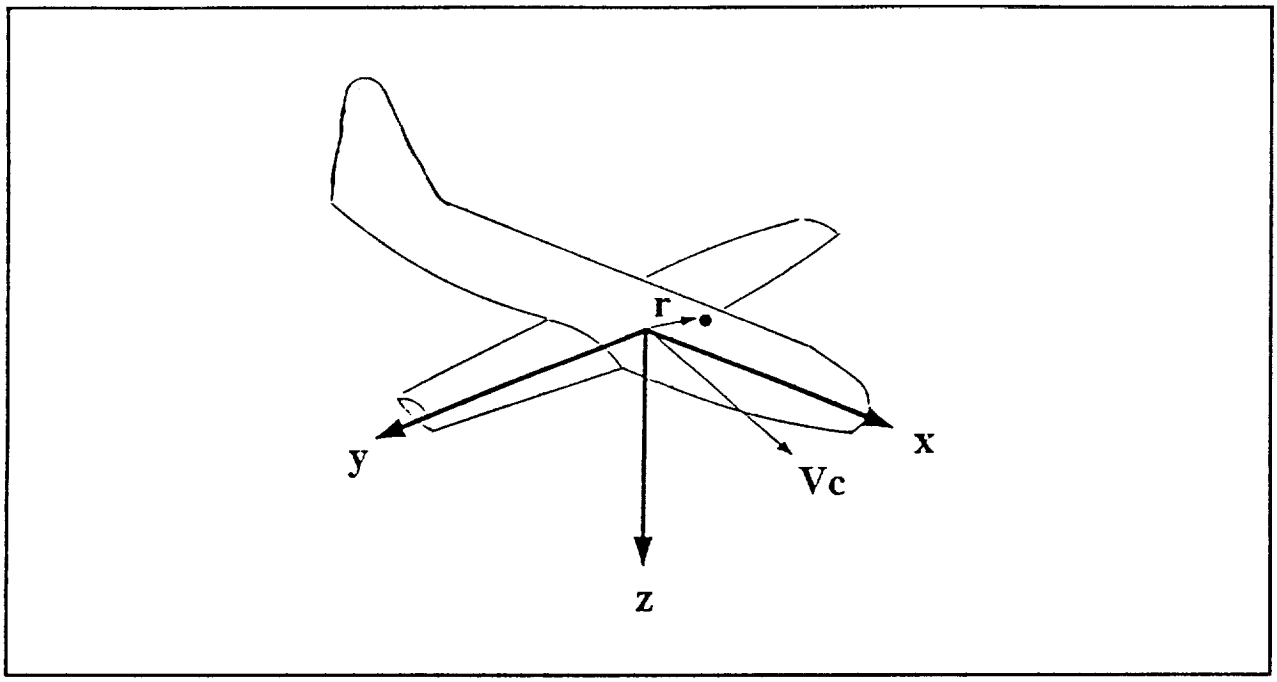

Figure 2 Body Axis System

From Figure 2, the velocity of the differential mass can be expressed as:

$$\vec{v} = \vec{v_c} + \frac{d\vec{r}}{dt} \tag{4}$$

Since the mass of the aircraft is assumed constant and the total mass of the aircraft is found by summing the mass elements, Newton's second law may be written as:

$$\sum \delta\vec{F} = \vec{F} = m\frac{d\vec{v}}{dt} + \frac{d^2}{dt^2}\sum(\vec{r})\delta m \tag{5}$$

The right hand side of Equation (5) equals zero since $\vec{r}$ is taken from the center of mass. Equation (5) now reduces to:

$$\vec{F} = m\frac{d\vec{v_c}}{dt} \tag{6}$$

The moment equation is developed in terms of the relative velocity of a mass element to the center of mass:

$$\vec{v} = \vec{v_c} + \frac{d\vec{r}}{dt} = \vec{v_c} + \vec{\omega} \times \vec{r} \tag{7}$$

where $\vec{\omega}$ is the angular velocity of the aircraft. Substituting this expression into the moment Equation (2), the total moment of momentum is:

$$\vec{H} = \sum (\vec{r})\delta m \times \vec{v_c} + \sum [\vec{r} \times (\vec{\omega} \times \vec{r})]\delta m \tag{8}$$

Again, the left hand side of Equation (8) equals zero and the moment of momentum equation reduces to:

$$\vec{H} = \sum [\vec{r} \times (\vec{\omega} \times \vec{r})]\delta m \tag{9}$$

A difficulty occurs if the reference is rotating, since the moment will vary with time. To eliminate this difficulty, a transformation of the reference frame is made to the body axis system (onto the aircraft). A vector $\vec{A}$ is transformed from a fixed system to a rotating coordinate system by:

$$\frac{d\vec{A}}{dt}\Big)fixed = \frac{d\vec{A}}{dt}\Big)rot. + \left[\vec{\omega} \times \vec{A}\right] \tag{10}$$

The force and moment equations, transformed into the body axis system, now become:

$$\vec{F} = m\frac{d\vec{v_c}}{dt} + m(\vec{\omega} \times \vec{v_c}) \tag{11}$$

$$\vec{M} = \frac{d\vec{H}}{dt} + \left(\vec{\omega} \times \vec{H}\right) \tag{12}$$

Vector Components and Scalar Equations

To obtain the time history results of Equations (11) and (12), it is necessary to express the vector equations into component form. The component forms of the forces, moments, gravity, linear and angular velocities are shown in Figure 3.[1] The corresponding equations are:

$$\begin{aligned}
\vec{F} &= F_x\vec{i} + F_y\vec{j} + F_z\vec{k} \\
\vec{M} &= L\vec{i} + M\vec{j} + N\vec{k} \\
\vec{g} &= g_x\vec{i} + g_y\vec{j} + g_z\vec{k} \\
\vec{\omega} &= P\vec{i} + Q\vec{j} + R\vec{k} \\
\vec{V_p} &= U\vec{i} + V\vec{j} + W\vec{k} \\
\vec{r} &= x\vec{i} + y\vec{j} + z\vec{k}
\end{aligned} \tag{13}$$

[1] Positive sense is in the direction of the arrows

Equation (11) can now be expanded into scalar form:

$$
\begin{aligned}
F_x + mg_x &= m\left(\dot{U} - VR + WQ\right) \\
F_y + mg_y &= m\left(\dot{V} + UR - WP\right) \\
F_z + mg_z &= m\left(\dot{W} - UQ + VP\right)
\end{aligned}
\tag{14}
$$

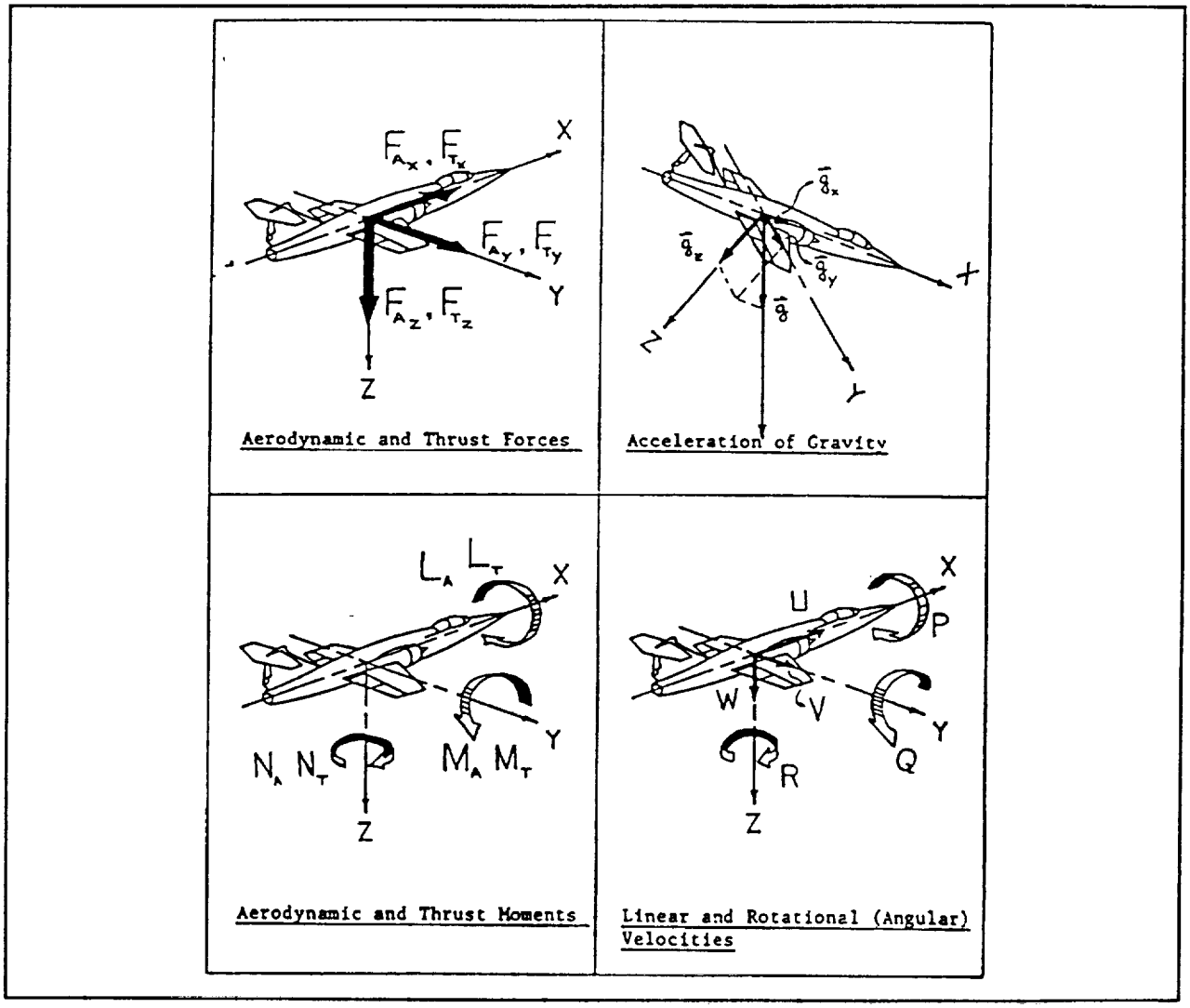

Figure 3 Vector Components (from Roskam [1])

After expanding Equation (9), the scalar components of the moment of momentum are:

$$
\begin{aligned}
H_x &= P\sum(y^2+z^2)\delta m - Q\sum(xy)\delta m - R\sum(xz)\delta m \\
H_y &= -P\sum(xy)\delta m + Q\sum(x^2+z^2)\delta m - R\sum(yz)\delta m \\
H_z &= -P\sum(xz)\delta m - Q\sum(yz)\delta m + R\sum(x^2+y^2)\delta m
\end{aligned} \tag{15}
$$

These equations can be expressed in terms of mass moments of inertia about the x, y, and z axes:

$$
\begin{aligned}
H_x &= I_{xx}P - I_{xy}Q - I_{xz}R \\
H_y &= -I_{xy}P + I_{yy}Q - I_{yz}R \\
H_z &= -I_{xz}P - I_{yz}Q + I_{zz}R
\end{aligned} \tag{16}
$$

Since, for most airplanes, the X-Z plane is a plane of symmetry, the moments of inertia for $I_{xy} = I_{yx} = zero$. With this assumption, and applying Equations (16) to the moment expression in Equation (12), the scalar moment equations can be written as:

$$
\begin{aligned}
L &= I_{xx}\dot{P} - I_{xz}\dot{R} - I_{xz}PQ + (I_{zz} - I_{yy})RQ \\
M &= I_{yy}\dot{Q} + (I_{xx} - I_{zz})PR + I_{xz}(P^2 - R^2) \\
N &= I_{zz}\dot{R} - I_{xz}\dot{P} + (I_{yy} - I_{xx})PQ + I_{xz}QR
\end{aligned} \tag{17}
$$

where L, M and N are the moments about the X, Y and Z axes, respectively.

Earth Fixed System and the Kinematic Equations

The force and moment equations are derived in the body-fixed axis system. But, the position of the aircraft must be described by the earth-fixed coordinate system. This is accomplished by three *consecutive* rotations (whose order is important). From Figure 4, the following rotations are made:

1. Rotate the $X_1Y_1Z_1$ body coordinate frame about the Z_1 axis over the **yaw** angle (Ψ) to the $X_2Y_2Z_2$ body coordinate frame.
2. Rotate the $X_2Y_2Z_2$ body coordinate frame about the Y_2 axis over the **pitch** angle (Θ) to the $X_3Y_3Z_3$ body coordinate frame.
3. Rotate the $X_3Y_3Z_3$ body coordinate frame about the X_3 axis over the **roll** angle (Φ) to the XYZ inertial coordinate frame.

These angles (yaw, pitch and roll) are known as the *Euler* angles.

The velocity components between the body-fixed coordinate system and the earth-fixed coordinate system are related by a set of orthogonal transformations (a more complete derivation may be found in [1] and [2]). These transformations are:

$$\begin{Bmatrix} \dot{x} \\ \dot{y} \\ \dot{z} \end{Bmatrix} = \begin{bmatrix} C_\Theta C_\Psi & S_\Phi S_\Theta C_\Psi - C_\Phi S_\Psi & C_\Phi S_\Theta C_\Psi + S_\Phi S_\Psi \\ C_\Theta S_\Psi & S_\Phi S_\Theta S_\Psi + C_\Phi C_\Psi & C_\Phi S_\Theta S_\Psi - S_\Phi C_\Psi \\ -S_\Theta & S_\Phi C_\Theta & C_\Phi C_\Theta \end{bmatrix} \begin{Bmatrix} U \\ V \\ W \end{Bmatrix} \tag{18}$$

where $C_\Phi \equiv \cos(\Phi)$, $S_\Psi \equiv \sin(\Psi)$, etc.

The kinematic equations relate the Euler angles (Ψ, Θ and Φ) and the angular velocities (P, Q and R). From Figure 4, $\vec{\omega}$ must equal the vector sum of the time rate of change of the Euler angles about the $\vec{k_1}$, $\vec{j_2}$, and $\vec{i_3}$ axes:

$$\vec{\omega} = \dot{\Psi}\vec{k_2} + \dot{\Theta}\vec{j_3} + \dot{\Phi}\vec{i} \tag{19}$$

Using transformations similar to Equation (18) and from Equation (13), the angular velocity may be written as:

$$\begin{aligned} \vec{\omega} = P\vec{i} + Q\vec{j} + R\vec{k} = \vec{i}\left(-\dot{\Psi}\sin\Theta + \dot{\Phi}\right) + \\ \vec{j}\left(\dot{\Psi}\cos\Theta\sin\Phi + \dot{\Theta}\cos\Phi\right) \\ \vec{k}\left(\dot{\Psi}\cos\Theta\cos\Phi - \dot{\Theta}\sin\Phi\right) \end{aligned} \tag{20}$$

Equating components, the kinematic equations become (in matrix form):

$$\begin{Bmatrix} P \\ Q \\ R \end{Bmatrix} = \begin{bmatrix} 1 & 0 & -\sin\Theta \\ 0 & \cos\Phi & \cos\Theta\sin\Phi \\ 0 & -\sin\Phi & \cos\Theta\cos\Phi \end{bmatrix} \begin{Bmatrix} \dot{\Phi} \\ \dot{\Theta} \\ \dot{\Psi} \end{Bmatrix} \tag{21}$$

The time histories of the Euler angles are determined by inverting the 3x3 matrix in Equation (21):

$$\begin{aligned} \dot{\Phi} &= P + Q\sin\Phi\tan\Theta + R\cos\Phi\tan\Theta \\ \dot{\Theta} &= Q\cos\Phi - R\sin\Phi \\ \dot{\Psi} &= (Q\sin\Phi + R\cos\Phi)\sec\Theta \end{aligned} \tag{22}$$

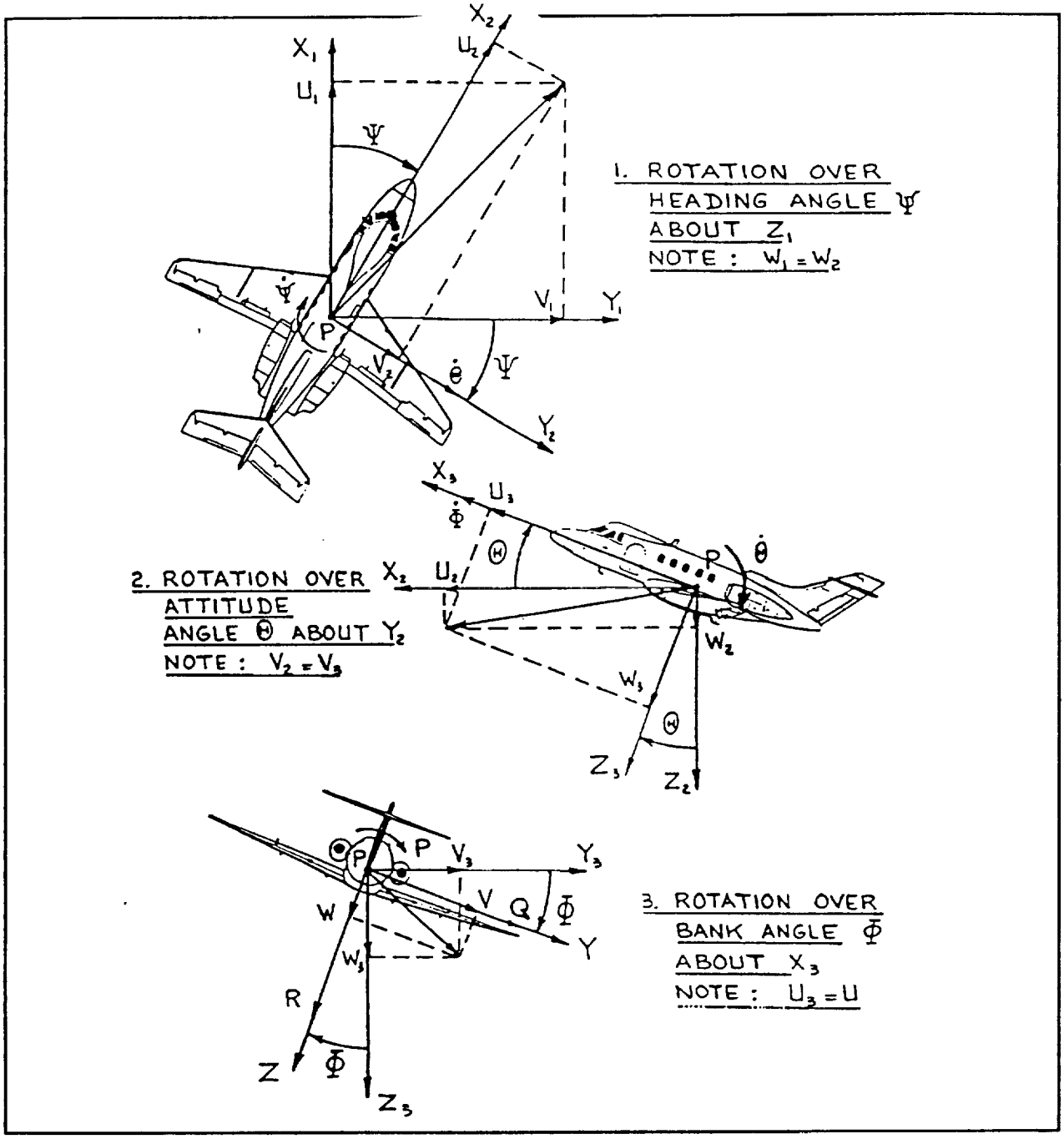

Figure 4 Rotation from Earth-Fixed to Body-Fixed Frame (from Roskam [1])

Aerodynamic Nomenclature

All forces and moments developed are based on the stability axes system defined by Figure 5. This system is utilized since experimental data from wind tunnel tests are presented in the stability axes. The stability axes are obtained by rotating the body axes (XYZ) about the $Y = Y_s$

axis. This is done over a rotational angle α (known as the angle of attack) until the body-fixed axis (X-axis) coincides with the free stream velocity vector ($\vec{V_{p_1}}$).

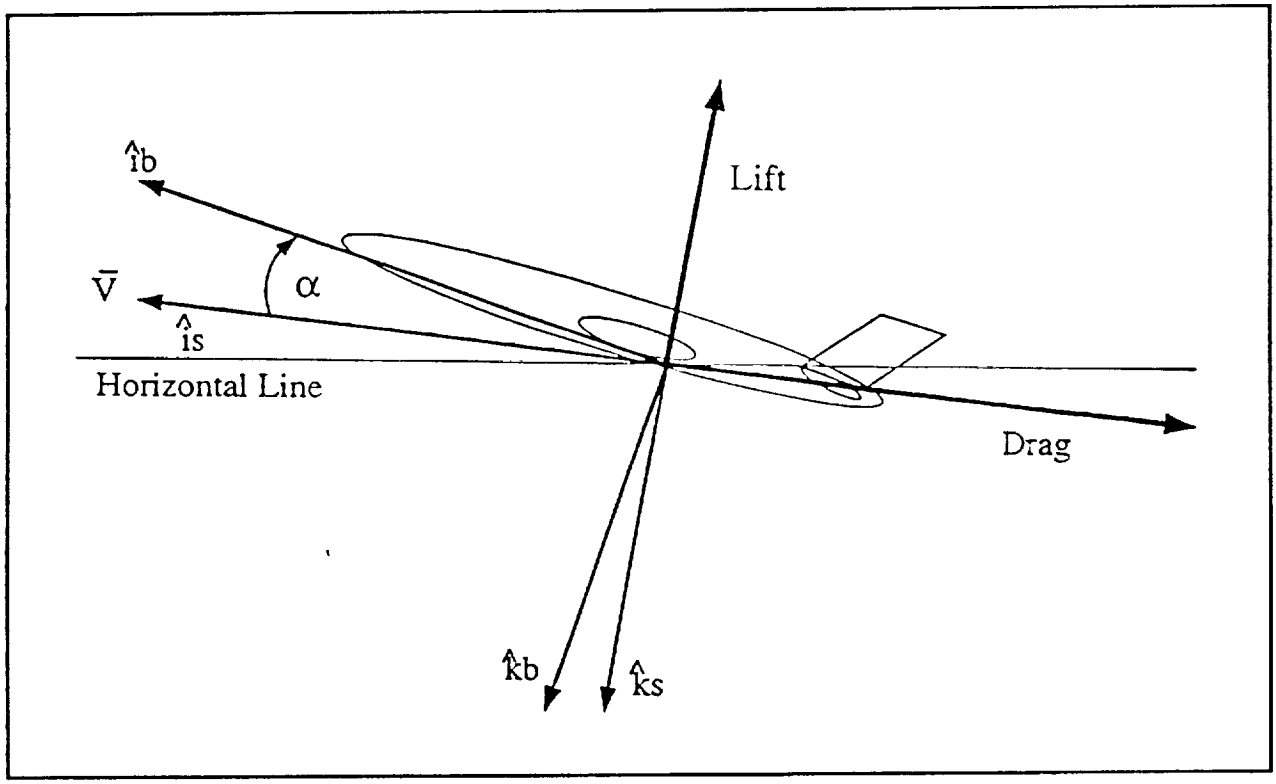

Figure 5 Stability Axis

The equation for the angle of attack is:

$$\alpha = \tan^{-1} \frac{W}{U} \tag{23}$$

The equation for the airspeed is:

$$V_p = \sqrt{(U^2 + V^2 + W^2)} \tag{24}$$

The flight path angle (γ) is the difference between the pitch angle and the angle of attack ($\gamma = \Theta - \alpha$). Figure 6 depicts the relationship between the different coordinate axes in the longitudinal plane.

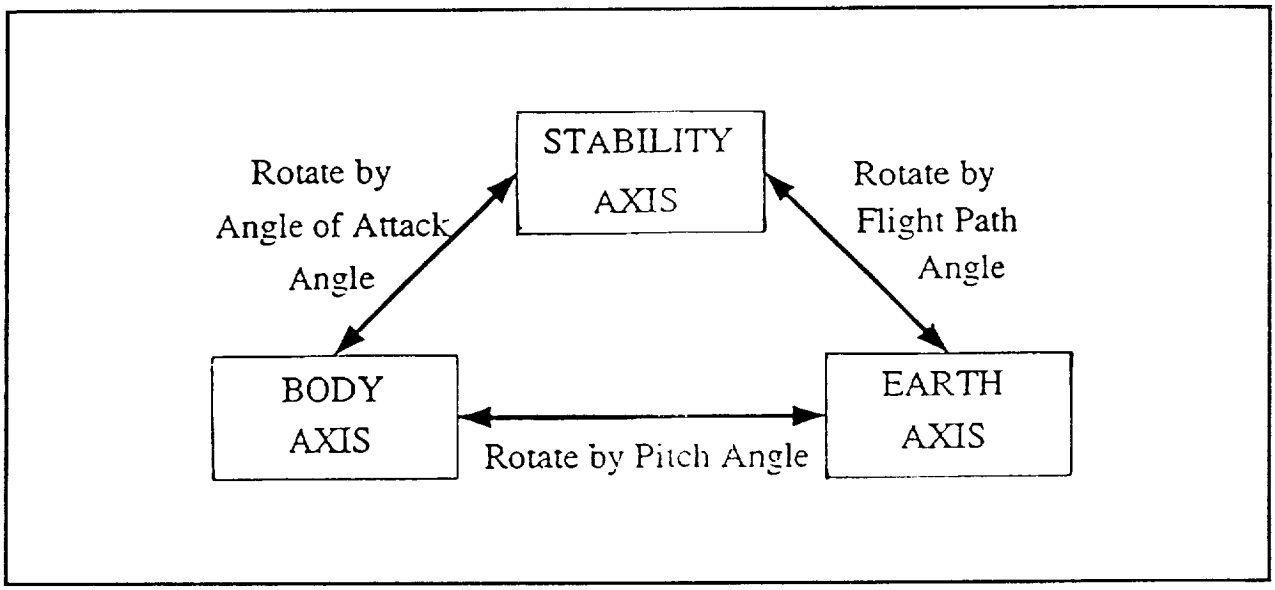

Figure 6 Relationship Between the Earth, Body and Stability Axis Frame

Forces and Moments

To simplify the analysis, all forces and moments are developed in the stability axis system. The force ($\vec{F}^s$) and moment ($\vec{M}^s$) components are:

$$\begin{aligned} \vec{F}^s &= F^s_{A_x}\vec{i}_s + F^s_{A_y}\vec{j}_s + F^s_{A_z}\vec{k}_s = -D\vec{i}_s + F_Y\vec{j}_s - L\vec{k}_s \\ \vec{M}^s &= L_A\vec{i}_s + M_A\vec{j}_s + N_A\vec{k}_s \end{aligned} \tag{25}$$

where D = Drag, L = Lift and F_Y = Sideforce. L_A, M_A and N_A are aerodynamic moments.

The steady state forces and moments for a straight line flight are assumed to depend only on angle of attack (α), sideslip angle (β), thrust and the control surface deflections of the elevator (δ_E), ailerons (δ_A), rudder (δ_R), and aerodynamic coefficients. These dimensionless coefficients are comprised of derivatives evaluated at constant Mach and Reynolds number (e.g.):

$$C_D = C_{D_0} + C_{D_\alpha}\alpha + C_{D_{\delta_E}}\delta_E \tag{26}$$

where:

- C_{D_0} = total airplane drag coefficient for $\alpha = \delta_E = 0$.
- $C_{D\alpha}$ = total airplane drag change with angle of attack for $\delta_E = 0$.
- $C_{D_{\delta_E}}$ = total airplane drag change with elevator angle for $\alpha = 0$.

A similar analysis is made for the remaining aerodynamic coefficients.

The aerodynamic forces and moments are expressed in terms of the dimensionless coefficients, flight dynamic pressure, characteristic length (for the moments only) and a reference area:

$$\begin{aligned} D &= C_D \bar{q} S = \left(C_{D_0} + C_{D_\alpha} \alpha + C_{D_{\delta_E}} \delta_E \right) \bar{q} S \\ F_Y &= C_{F_Y} \bar{q} S = \left(C_{Y_\beta} \beta + C_{Y_{\delta_A}} \delta_A + C_{Y_{\delta_R}} \delta_R \right) \bar{q} S \\ L &= C_L \bar{q} S = (C_{L_0} + C_{L_\alpha} \alpha + C_{L_{\delta E}} \delta_E) \bar{q} S \end{aligned} \tag{27}$$

$$\begin{aligned} L_A &= C_l \bar{q} S b \\ &= \left(C_{l_\beta} \beta + C_{l_{\delta_A}} \delta_A + C_{l_{\delta_R}} \delta_R + C_{l_P} \frac{Pb}{2U_s} + C_{l_R} \frac{Rb}{2U_s} \right) \bar{q} S b \\ M_A &= C_M \bar{q} S \bar{c} \\ &= \left(C_{M_0} + C_{M_\alpha} \alpha + C_{M_{\delta_E}} \delta_E + C_{M_Q} \frac{Q\bar{c}}{2U_s} \right) \bar{q} S \bar{c} \\ N_A &= C_N \bar{q} S b \\ &= \left(C_{N_\beta} \beta + C_{N_{\delta_A}} \delta_A + C_{N_{\delta_R}} \delta_R + C_{N_P} \frac{Pb}{2U_s} + C_{N_R} \frac{Rb}{2U_s} \right) \bar{q} S b \end{aligned} \tag{28}$$

The flight dynamic pressure is :

$$\bar{q} = \frac{1}{2} \rho U_s^2 \tag{29}$$

where ρ is the air density and U_s is the aircraft's airspeed.

The aircraft thrust vector is also divided into components:

$$\begin{aligned} F_{T_x}^s &= T \cos(\alpha) \\ F_{T_y}^s &= 0 \\ F_{T_z}^s &= -T \sin(\alpha) \\ L_T^s &= 0 \\ M_T^s &= -T d_T \\ N_T^s &= 0 \end{aligned} \tag{30}$$

where d_T is the moment arm of thrustline.

For a *trimmed* airplane, the forces and moments acting on it are in equilibrium. This is accomplished when the pitching moment equals zero and when the lift equals the airplane

weight. Using Equations (27) and (28):

$$\begin{aligned} 0 &= \left(C_{M_0} + C_{M_\alpha}\alpha + C_{M_{\delta_E}}\delta_E\right) \\ \frac{mg}{\bar{q}S} = C_{L_{trim}} &= \left(C_{L_0} + C_{L_\alpha}\alpha + C_{L_{\delta_E}}\delta_E\right) \end{aligned} \tag{31}$$

Solving these equations for α and δ_E determines the trim value for the angle of attack and the trim elevator setting:

$$\alpha_{trim} = \frac{C_{L_{trim}}C_{M_{\delta_E}} - C_{L_0}C_{M_{\delta_E}} + C_{L_{\delta_E}}C_{M_0}}{C_{L_\alpha}C_{M_{\delta_E}} - C_{L_{\delta_E}}C_{M_\alpha}} \tag{32}$$

$$\delta_{E_{trim}} = \frac{C_{L_{trim}}C_{M_\alpha} - C_{L_0}C_{M_\alpha} + C_{L_\alpha}C_{M_0}}{C_{L_{\delta_E}}C_{M_\alpha} - C_{L_\alpha}C_{M_{\delta_E}}} \tag{33}$$

Combining the rigid body equations and the aircraft kinematic equations yields a full set of flight dynamics equations that describe any aircraft flight path or motion. To accomplish this, all forces must first be transformed from the stability axis system to the body axis system. From Figure 5:

$$\begin{aligned} F_x^b &= -D\cos(\alpha) + L\sin(\alpha) + T\cos(\alpha) \\ F_y^b &= F_y^s \\ F_z^b &= -D\sin(\alpha) - L\cos(\alpha) + T\sin(\alpha) \end{aligned} \tag{34}$$

The force equations (14) are then solved in terms of the linear velocity rates ($\dot{U}$, $\dot{V}$ and $\dot{W}$). Also, the moment equations (17) are solved in terms of the angular velocity rates ($\dot{P}$, $\dot{Q}$ and $\dot{R}$). To simplify the analysis, let:

$$\begin{aligned} k_1 &= I_{XZ}(I_{YY} - I_{XX}) \\ k_2 &= I_{ZZ}(I_{ZZ} - I_{YY}) \\ k_3 &= I_{XZ}(I_{ZZ} - I_{YY}) \\ k_4 &= I_{XX}(I_{YY} - I_{XX}) \end{aligned} \tag{35}$$

The full flight dynamic motions are now expressed as a 12^{th} order set of nonlinear differential equations (three of which are simple integrations of the linear velocities to yield linear positions). These equations can now be integrated to yield flight trajectories, after a transformation is made

to the earth-fixed coordinate system by Equation (18), of any variable (e.g. plane altitude, airspeed, etc).

$$\dot{U} = -g\sin(\Theta) + \frac{F_x^b}{m} + VR - WQ \tag{36}$$

$$\dot{V} = g\sin(\Phi)\cos(\Theta) + \frac{F_y^b}{m} - UR + WP \tag{37}$$

$$\dot{W} = g\cos(\Phi)\cos(\Theta) + \frac{F_z^b}{m} + UQ - VP \tag{38}$$

$$\dot{P} = \frac{I_{XZ}N_A + I_{ZZ}L_A - k_1PQ - I_{XZ}^2QR + I_{XZ}I_{ZZ}PQ - k_2RQ}{I_{XX}I_{ZZ} - I_{XZ}^2} \tag{39}$$

$$\dot{Q} = \frac{M_A - (I_{XX} - I_{ZZ})PQ - I_{XZ}(P^2 - R^2)}{I_{YY}} \tag{40}$$

$$\dot{R} = \frac{I_{XX}N_A + I_{XZ}L_A + I_{XZ}^2PQ - k_3RQ - k_4PQ - I_{XX}I_{XZ}QR}{I_{ZZ}I_{XX} - I_{XZ}^2} \tag{41}$$

$$\dot{\Theta} = Q\cos\Phi - R\sin\Phi \tag{42}$$

$$\dot{\Psi} = (Q\sin\Phi + R\cos\Phi)\sec\Theta \tag{43}$$

$$\dot{\Phi} = P + Q\sin\Phi\tan\Theta + R\cos\Phi\tan\Theta \tag{44}$$

Table 1 Flight Dynamic Equations

The full flight dynamic equations in Table 1 may be linearized into second order differential equations by utilizing small disturbance theory. This theory applies to small deviations (for angle of attack, sideslip and control surface deflections, etc.) relative to some steady state flight condition. For an automatic landing system, this assumption is valid since only small angle deviations caused by turbulence or control variables are encountered. This theory is also useful in analyzing the stability of an autopilot by using longitudinal transfer functions.

Small Perturbation Equations (stability axis)

Perturbed state equations are derived by replacing all motion variables by a steady state value and a perturbation:

$$\begin{aligned} U &= U_0 + \Delta U & V &= V_0 + \Delta V & W &= W_0 + \Delta W \\ P &= P_0 + \Delta P & Q &= Q_0 + \Delta Q & R &= R_0 + \Delta R \\ \Psi &= \Psi_0 + \Delta\Psi & \Theta &= \Theta_0 + \Delta\Theta & \Phi &= \Phi_0 + \Delta\Phi \end{aligned} \tag{45}$$

This also applies to all forces and moments:

$$\begin{aligned} F_x &= F_{x_0} + \Delta F_x & F_y &= F_{y_0} + \Delta F_y & F_z &= F_{z_0} + \Delta F_z \\ M &= M_0 + \Delta M & L &= L_0 + \Delta L & N &= N_0 + \Delta N \end{aligned} \tag{46}$$

The change in forces and moments can be expressed in terms of the perturbation variables by using a Taylor series expansion:

$$\begin{aligned} \Delta F_x &= \frac{\partial F_x}{\partial U}\Delta U + \frac{\partial F_x}{\partial W}\Delta W + \frac{\partial F_x}{\partial \delta_E}\Delta\delta_E + \frac{\partial F_x}{\partial \delta_T}\Delta\delta_T \\ \Delta F_y &= \frac{\partial F_y}{\partial V}\Delta V + \frac{\partial F_y}{\partial P}\Delta P + \frac{\partial F_y}{\partial R}\Delta R + \frac{\partial F_y}{\partial \delta_R}\Delta\delta_R \\ \Delta F_z &= \frac{\partial F_z}{\partial U}\Delta U + \frac{\partial F_z}{\partial W}\Delta W + \frac{\partial F_z}{\partial Q}\Delta Q + \frac{\partial F_z}{\partial \delta_E}\Delta\delta_E + \frac{\partial F_z}{\partial \delta_T}\Delta\delta_T \\ \Delta M &= \frac{\partial M}{\partial U}\Delta U + \frac{\partial M}{\partial W}\Delta W + \frac{\partial M}{\partial Q}\Delta Q + \frac{\partial M}{\partial \delta_E}\Delta\delta_E + \frac{\partial M}{\partial \delta_T}\Delta\delta_T \\ \Delta L &= \frac{\partial L}{\partial V}\Delta V + \frac{\partial L}{\partial P}\Delta P + \frac{\partial L}{\partial R}\Delta R + \frac{\partial L}{\partial \delta_R}\Delta\delta_R + \frac{\partial L}{\partial \delta_A}\Delta\delta_A \\ \Delta N &= \frac{\partial N}{\partial V}\Delta V + \frac{\partial N}{\partial P}\Delta P + \frac{\partial N}{\partial R}\Delta R + \frac{\partial N}{\partial \delta_R}\Delta\delta_R + \frac{\partial N}{\partial \delta_A}\Delta\delta_A \end{aligned} \tag{47}$$

The partial derivatives in Equation (47) are called the *stability derivatives.* For convenience, these derivatives are divided by the aircraft mass. These new symbols are defined as *dimensional stability derivatives* (e.g.):

$$X_u = \left(\frac{F_x}{\partial U}\right)/(m) \qquad X_w = \left(\frac{F_x}{\partial W}\right)/(m) \tag{48}$$

Replacing the forces and moments with Equation (25) the longitudinal dimensional stability derivatives, in the stability axis system, become:

$$X_u = \frac{-2C_{D_0}\bar{q}_0 S}{mU_0} \qquad X_{\delta_E} = \frac{-2C_{D_{\delta_E}}\bar{q}_0 S}{m} \qquad Z_u = \frac{-2C_{L_0}\bar{q}_0 S}{mU_0}$$

$$Z_{\dot{\alpha}} = \frac{-C_{L_{\dot{\alpha}}}\bar{q}_0 S\bar{c}}{2mU_0} \qquad Z_q = \frac{-C_{L_Q}\bar{q}_0 S\bar{c}}{2mU_0} \qquad Z_{\delta_E} = \frac{-C_{L_{\delta_E}}\bar{q}_0 S}{m}$$

$$M_u = \frac{2C_{M_0}\bar{q}_0 S\bar{c}}{I_{YY}U_0} \qquad M_\alpha = \frac{-C_{M_\alpha}\bar{q}_0 S\bar{c}}{I_{YY}} \qquad M_{\dot{\alpha}} = \frac{C_{M_{\dot{\alpha}}}\bar{q}_0 S\bar{c}^2}{2I_{YY}U_0} \tag{49}$$

$$M_q = \frac{C_{M_Q}\bar{q}_0 S\bar{c}^2}{2I_{YY}U_0} \qquad M_{\delta_E} = \frac{C_{M_{\delta_E}}\bar{q}_0 S\bar{c}}{I_{YY}} \qquad M_{T_\alpha} = \frac{C_{M_{T_\alpha}}\bar{q}_0 S\bar{c}}{I_{YY}}$$

$$X_\alpha = \frac{-(C_{D_\alpha} - C_{L_0})\bar{q}_0 S}{m} \qquad Z_\alpha = \frac{-(C_{L_\alpha} + C_{D_0})\bar{q}_0 S}{m}$$

These dimensional stability derivatives, along with the force and moment perturbation equations, can now be evaluated into the full flight dynamic equations (Table 1). To simplify the analysis, for small angle deflections, let:

$$\begin{aligned} \cos\Theta &\approx 1.0 \\ \sin\Theta &\approx \Theta \end{aligned} \tag{50}$$

Taking a Laplace Transformation of the resulting equations determines the longitudinal transfer functions with the elevator setting (δ_E) as the input and the horizontal velocity component (U), angle of attack (α) and pitch angle (Θ) as the output variables. These longitudinal transfer functions, in matrix form, are:

$$\begin{Bmatrix} A_{11} & A_{12} & A_{13} \\ A_{21} & A_{22} & A_{23} \\ A_{31} & A_{32} & A_{33} \end{Bmatrix} \begin{Bmatrix} \frac{U(s)}{\delta_E(s)} \\ \frac{\alpha(s)}{\delta_E(s)} \\ \frac{\Theta(s)}{\delta_E(s)} \end{Bmatrix} = \begin{Bmatrix} X_{\delta_E} \\ Z_{\delta_E} \\ M_{\delta_E} \end{Bmatrix} \tag{51}$$

where:

$$
\begin{aligned}
A_{11} &= (s - X_u) \\
A_{12} &= -X_\alpha \\
A_{13} &= g \cos \Theta_0 \\
A_{21} &= -Z_u \\
A_{22} &= s(U_0 - Z_{\dot{\alpha}}) - Z_\alpha \\
A_{23} &= -(Z_q + U_0)s + g \sin \Theta_0 \\
A_{31} &= -(M_u + M_{T_u}) \\
A_{32} &= -(sM_{\dot{\alpha}} + M_\alpha) \\
A_{33} &= s^2 - sM_q
\end{aligned}
\tag{52}
$$

Taking the inverse of Equation (51) yields the transfer functions for the longitudinal mode. Using Cramer's Rule, the denominator of the transfer functions is a fourth order polynomial. The roots of this polynomial form the *characteristic equation* and determine the stability of an aircraft. The characteristic equation is represented by two oscillatory modes of motion (short period and phugoid).

Short and Long Period Approximations

The longitudinal motion of an aircraft is determined by two modes. The first is the *short period* mode. This is characterized by a highly damped, high natural frequency oscillation at approximately constant speed ($\Delta U \approx 0$). The other mode is the long period or *phugoid* mode. This is caused by a gradual change between potential and kinetic energy and is characterized by a low damped, low natural frequency oscillation at approximately constant angle of attack ($\Delta \alpha \approx 0$). Both modes are determined by the characteristic roots of Equation (51). The concept of these modes is illustrated in Figure 7.

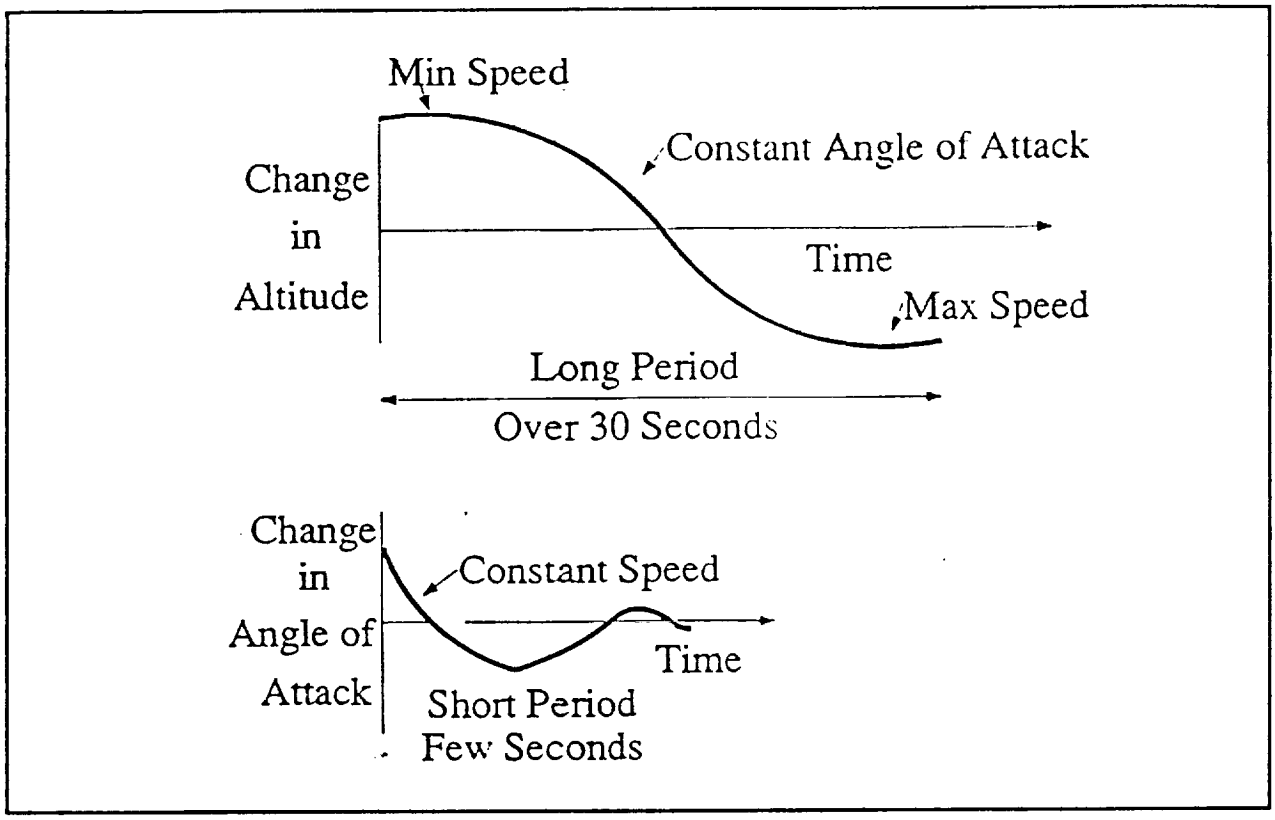

Figure 7 Short Period and Phugoid Modes

The short period mode is obtained by approximately neglecting the velocity term in Equation (51). This equation now reduces to:

$$\begin{Bmatrix} sU_0 - Z_\alpha & -sU_0 \\ -M_{\dot{\alpha}} - M_\alpha & s^2 - sM_q \end{Bmatrix} \begin{Bmatrix} \frac{\alpha(s)}{\delta_E(s)} \\ \frac{\Theta(s)}{\delta_E(s)} \end{Bmatrix} = \begin{Bmatrix} Z_{\delta_E} \\ M_{\delta_E} \end{Bmatrix} \tag{53}$$

Applying the inverse to this equation:

$$\begin{aligned} \frac{\alpha(s)}{\delta_E(s)} &= \frac{sZ_{\delta_E} + (M_{\delta_E}U_0 - M_qZ_{\delta_E})}{s\{s^2U_0 - s(M_qU_0 + Z_\alpha + U_0M_{\dot{\alpha}}) + (Z_\alpha M_q - M_\alpha U_0)\}} \\ \frac{\Theta(s)}{\delta_E(s)} &= \frac{s(U_0M_{\delta_E} + Z_{\delta_E}M_{\dot{\alpha}}) + (M_\alpha Z_{\delta_E} - Z_\alpha M_{\delta_E})}{s\{s^2U_0 - s(M_qU_0 + Z_\alpha + U_0M_{\dot{\alpha}}) + (Z_\alpha M_q - M_\alpha U_0)\}} \end{aligned} \tag{54}$$

Comparing the denominator of this equation to the standard frequency form of $(s^2 + s2\zeta\omega_{n_{SP}} + \omega_{n_{SP}}^2)$, the natural frequency and damping ratio of the short period mode are:

$$\omega_{n_{SP}} = \sqrt{\frac{Z_\alpha M_q}{U_0} - M_\alpha}$$

$$\zeta_{SP} = \frac{-(M_q U_0 + Z_\alpha + M_{\dot{\alpha}} U_0)}{2\omega_{n_{SP}} U_0} \tag{55}$$

The phugoid approximation is derived by neglecting the angle of attack term in Equation (51). The resulting equations for this mode become:

$$\frac{U(s)}{\delta_E(s)} = \frac{Z_{\delta_E} U_0 g}{(s^2 U_0 - s X_u U_0 - Z_u g)}$$

$$\frac{\Theta(s)}{\delta_E(s)} = \frac{-Z_{\delta_E} U_0 (s - X_u)}{(s^2 U_0 - s X_u U_0 - Z_u g)} \tag{56}$$

The natural frequency and damping ratio for the phugoid mode are:

$$\omega_{n_P} = \sqrt{\frac{-Z_u g}{U_0}}$$

$$\zeta_P = \frac{-X_u}{2\omega_{n_P}} \tag{57}$$

The combination of the short period and phugoid modes describes the complete longitudinal aircraft motion (i.e.):

$$\frac{\Theta(s)}{\delta_E(s)} = \frac{k_{\Theta\delta}(T_{\Theta_1} s + 1)(T_{\Theta_2} s + 1)}{\left(\frac{s^2}{\omega_{n_{SP}}^2} + \frac{2\zeta_{SP}}{\omega_{n_{SP}}} + 1\right)\left(\frac{s^2}{\omega_{n_P}^2} + \frac{2\zeta_P}{\omega_{n_P}} + 1\right)} \tag{58}$$

REFERENCES

[1] Roskam, J., Aircraft Flight Dynamics and Automatic Control, Part I and II, Roskam Aviation and Engineering Corporation, U.S., 1979.

[2] Nelson, R.C., Flight Stability and Automatic Control, McGraw Hill, 1987.